Theoretical study on removal rate and surface roughness in grinding a RB-SiC mirror with a fixed abrasive

Xu Wang[1,2] and Xuejun Zhang[1,*]

[1]Key Laboratory of Optical System Advanced Manufacturing Technology, Chinese Academy of Science, Changchun 130033, China

[2]Graduate School of the Chinese Academy of Sciences, Beijing 100039, China

*Corresponding author: zxj@ciomp.ac.cn

Received 6 November 2008; revised 14 December 2008; accepted 18 December 2008; posted 5 January 2009 (Doc. ID 103784); published 2 February 2009

This paper is based on a microinteraction principle of fabricating a RB-SiC material with a fixed abrasive. The influence of the depth formed on a RB-SiC workpiece by a diamond abrasive on the material removal rate and the surface roughness of an optical component are quantitatively discussed. A mathematical model of the material removal rate and the simulation results of the surface roughness are achieved. In spite of some small difference between the experimental results and the theoretical anticipation, which is predictable, the actual removal rate matches the theoretical prediction very well. The fixed abrasive technology's characteristic of easy prediction is of great significance in the optical fabrication industry, so this brand-new fixed abrasive technology has wide application possibilities. © 2009 Optical Society of America

OCIS codes: 220.0220, 220.4000, 220.4610, 220.5450.

1. Introduction

For the new generation Earth observation optical system, high resolution is required, and the system needs to be able to see a large swatch of Earth at the same time. The optical system that is developed must have large diameter, off axis capability and be lightweight to satisfy the technical demands of high quality, high resolution, and large viewing area in the development of national defense technology in China. A high quality and light optical mirror is the key component of an optical remote sensing camera. Hence, technical demands bring forward extremely strict properties about mirror material.

Properties of several materials used for telescopes are displayed in Table 1. The excellent mechanical and thermal performance of SiC in Table 1 make it a proper mirror material for a space telescope, especially because RB-SiC has perfect specific stiffness and better surface shape stability. Therefore, RB-SiC is a superior optical mirror material that has great potential (see details in [1]). However, the advantages of its application in a space telescope are also the disadvantages in the fabrication of a RB-SiC mirror. It is very difficult to polish RB-SiC because of its high hardness, and there is unstable fabrication accuracy, lower fabrication efficiency, and high cost, especially when applying traditional loose abrasive technology in fabrication. Therefore, it was important to find better solutions to the above-mentioned problems.

In the 1970s the development of fixed abrasive technology overcame most of the disadvantages faced in traditional loose abrasive technology at low fabrication velocity. Since then, fixed abrasive technology has improved qualitatively so that an excellent and lightweight RB-SiC workpiece can be manufactured. The characteristic of accurate fabrication of fixed

0003-6935/09/050904-07$15.00/0

Table 1. Properties of Several Materials Used for Telescope

	Young's Modulus (Gpa)	Density (g/cm^3)	Thermal Expansion (ppm/K)	Thermal Conductivity (W/mK)
RB-SiC	330	3.04	2.4	170
Zerodur	92	2.53	−0.09	1.6
Be	287	1.85	11.3	216
Fused silica	73	2.19	0.50	1.40

abrasives makes it possible to exactly describe the fabrication process with a theoretical model. This predictability is the basis for manufacturing a large-diameter RB-SiC workpiece by computer-controlled optical fabrication. This paper is based on the reasons mentioned above, and fabricating a RB-SiC workpiece with fixed abrasive technology is adopted for the first time to the best of our knowledge. It begins from theoretical analysis in Section 2 and in Subsection 3.A and also validates the feasibility of fabricating reaction bonded SiC with fixed abrasive technology.

2. Theoretical Models

Usually, fixed abrasive technology consists of a diamond abrasive, a special resin, and an additive, which are combined in a formation called a pellet. In the fabrication process, pellets are glued onto the polishing pad with a special adhesive, which makes it easy for fabrication. Because the position of the diamond abrasive is fixed in the pellet and the concentration of abrasive is invariable, it is suitable for mathematical modeling.

A. Calculation of Abrasive Number in the Unit Surface Area of the Pellet

Supposing that the concentration of the abrasive in the pellet is ξ (in percent) and the diameter of the diamond abrasive is D (μm), the abrasive number in the unit surface area of the pellet will be

$$m = \frac{4\xi^{\frac{2}{3}}}{\pi D^2}. \tag{1}$$

The height of an abrasive outcropped from the resin is a, which is in uniformity distribution. Supposing that when $a > D/2$, the abrasive will fall off. So the distribution density function of a is

$$f(a) = \begin{cases} \frac{1}{a_{\max}} & (0 < a < a_{\max} < \frac{D}{2}) \\ 0 & (\text{else}) \end{cases}. \tag{2}$$

The distribution probability is denoted as

$$P\{a < x\} = \int_0^x \frac{1}{a_{\max}} \mathrm{d}a = \frac{x}{a_{\max}}, \tag{3}$$

so the number of abrasives with height bigger than x in the unit area of pellet is

$$m_1 = \frac{4\xi^{\frac{2}{3}}}{\pi D^2}\left(1 - \frac{x}{a_{\max}}\right). \tag{4}$$

B. Calculation of the Indentation Depth of the Abrasive

According to the model in [2], Eq. (5), which is used to distinguish the contact type between resin and abrasive, is introduced:

$$\delta_{r-c} = \left(\frac{3\pi k_r H_r}{4E_{r-c}}\right)^2 \left(\frac{D}{2}\right), \tag{5}$$

where

$$\frac{1}{E_{r-c}} = \frac{1-\nu_r{}^2}{E_r} + \frac{1-\nu_c^2}{E_c}, \tag{6}$$

H_r and k_r are the surface hardness and the mean contact pressure factor of the pellet, respectively, and E_{r-c} is the reduced Young's modulus of the resin and the diamond abrasive.

The parameters in Eqs. (5) and (6) take the following values:

$H_r = 1.717\,\text{Gpa}$, $E_r = 686.6\,\text{Mpa}$, $\nu_r = 0.4$, $E_c = 1144\,\text{Gpa}$, $\nu_c = 0.1$, and $k_r = 0.4$.

Then

$$\delta_{r-c} = 2.77D. \tag{7}$$

Equation (7) shows that when the indentation into the resin by a diamond abrasive particle is more than 2.77 times the abrasive diameter, the contact type between the resin and the diamond abrasive is plastic. But in a real situation, the indentation is less than the abrasive diameter, so the contact type is elastic deformation.

Equation (8), which is used to distinguish the contact type between the workpiece and the abrasive, is also introduced:

$$\delta_{\text{sic}-c} = \left(\frac{3\pi k_{\text{sic}} H_{\text{sic}}}{4E_{\text{sic}-c}}\right)^2 \left(\frac{D}{2}\right), \tag{8}$$

where H_{sic} and k_{sic} are the surface hardness and the mean contact pressure factor of the pellet, respectively, $E_{\text{sic}-c}$ is the reduced Young's modulus of the RB-SiC workpiece and the diamond abrasive.

The parameters in Eq. (8) take the following values:

$H_{\text{sic}} = 30\,\text{Gpa}$, $E_{\text{sic}} = 330\,\text{Gpa}$, $\nu_{\text{sic}} = 0.2$, $E_c = 1144\,\text{Gpa}$, $\nu_c = 0.1$, and $k_{\text{sic}} = 0.4$.

Then

$$\delta_{\text{sic}-c} = 0.0057D. \tag{9}$$

Equation (9) shows that once the indentation into the RB-SiC workpiece by a particle of the diamond abrasive is less than 0.0057 times the size of the abrasive, the contact type between the RB-SiC

workpiece and the abrasive is elastic. If the abrasive diameter is $1.5\,\mu$m, $\delta_{sic-c} = 8.55$ nm, which is much smaller than abrasive diameter. The contact type between the RB-SiC workpiece and the abrasive is likely to be plastic in the fabrication process.

So the following equation is derived from elastic mechanics: the contact force between the diamond abrasive in the pellet and the RB-SiC workpiece is denoted as

$$F_{fw} = H_w \pi D \delta_w. \tag{10}$$

The contact force between the diamond abrasive and the resin in the pellet is

$$F_{fp} = \frac{4}{3} E_{fp} \left(\frac{D}{2}\right)^{\frac{1}{2}} \delta_p^{\frac{3}{2}}, \tag{11}$$

where E_{fp} is the reduced Young's modulus of the diamond abrasive and the resin, H_w is the hardness of the RB-SiC workpiece, and δ_p and δ_w are the indentation depths on the resin and the workpiece under certain pressure, respectively.

The microinteraction model is displayed in Fig. 1. Because the model is used in fixed abrasive technology, we have been on the assumption that a, which is the height of abrasive outcropped from the resin, is less than $D/2$, If $a > D/2$, the abrasive will fall off. So for fixed abrasive technology, when the abrasive contacts the RB-SiC workpiece fully, the relationship between δ_p and δ_w is revealed by $\delta_p + \delta_w = a$, where $0 < a < D/2$. In Eq. (2), we can see that the concept of a is introduced and is kept to the statistic of uniformity distribution. A model that includes the concept of statistic probability can better describe the fabrication process of fixed abrasive technology.

The principle of force balance $F_{fp} = F_{fw}$ is used in the model, so Eq. (12) is obtained:

$$\frac{4}{3} E_{fp} \left(\frac{D}{2}\right)^{\frac{1}{2}} (a - \delta_w)^{\frac{3}{2}} = H_w \pi D \delta_w. \tag{12}$$

According to Eq. (12), finally

$$\delta_w^3 + \left(\frac{9 H_w^2 \pi^2 D}{8 E_{fp}^2} - 3a\right) \delta_w^2 + 3a^2 \delta_w - a^3 = 0. \tag{13}$$

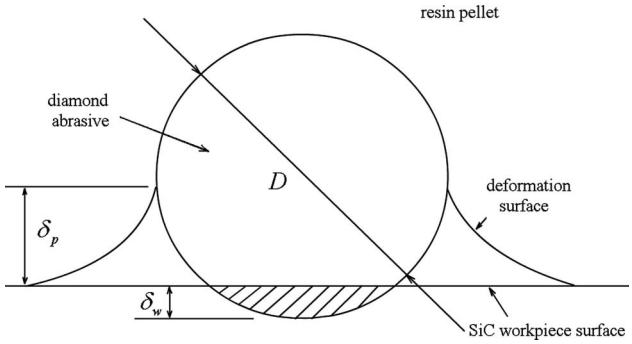

Fig. 1. Model of microinteraction between a diamond fixed abrasive and a workpiece.

The indentation depth on the RB-SiC workpiece fabricated by a diamond abrasive is gained when the δ_w in Eq. (13) is solved.

C. Theoretical Calculation of Material Removal Rate

The material removal rate is defined as the average material removal height on a workpiece in unit time. Figure 2 is an enlarged picture of the contact area between a single diamond abrasive and a RB-SiC workpiece.

For the integrality of the derived process of the formula in the paper, Eqs. (9)–(14) are introduced from [3].

For single diamond abrasive, the material removal in time t is

$$\Delta G = K \cdot \Delta S \cdot V \cdot t, \tag{14}$$

where K is constant, t is the polishing time, ΔS is the cross section area of the groove in the workpiece formed by a single diamond abrasive, and V is the diamond abrasive instantaneous sliding velocity.

According to the definition of material removal rate, the equation is denoted as

$$\Delta Z = \frac{\Delta G N_a}{A_n t} = \frac{K \cdot \Delta S \cdot V \cdot N_a}{A_n}, \tag{15}$$

where N_a is the number of abrasives whose height is outcropped from the resin in area A_t, defined as $N_a = A_t m_1$. A_t is the total real contact area between the abrasive in the pellet and the workpiece, A_n is the macroscopical contact area between the pellet and the workpiece. The constant K in Eq. (14) is derived from Rabinowicz theory in [4]:

$$K = \frac{3}{\pi} \tan\theta \approx \frac{3}{\pi} \frac{\delta_w}{r} \approx \frac{3}{\pi} \frac{\delta_w}{(D\delta_w)^{\frac{1}{2}}} = \frac{3}{\pi} \left(\frac{\delta_w}{D}\right)^{\frac{1}{2}}. \tag{16}$$

According to the relationship of parameters in Fig. 2, the expression of ΔS is denoted as

$$\Delta S = \frac{1}{2} \delta_w (2r), \tag{17}$$

where

$$r = \left(\left(\frac{D}{2}\right)^2 - \left(\frac{D}{2} - \delta_w\right)^2\right)^{\frac{1}{2}} = (\delta_w D - \delta_w^2)^{\frac{1}{2}}. \tag{18}$$

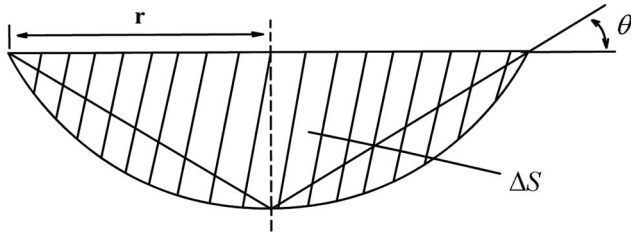

Fig. 2. Sketch of the contact area between a single abrasive and a workpiece.

Because of $\delta_w \ll D$, the simplification of ΔS is

$$\Delta S \approx \delta_w^{\frac{3}{2}} D^{\frac{1}{2}}. \tag{19}$$

With the combination of Eqs. (4), (15), and (19), according to the result of Eq. (13) and the concept of statistic probability, finally we have the expression of the maximum removal rate:

$$\Delta Z = \frac{12\xi^{\frac{2}{3}}}{\pi^2 D^2} V A_t^* \delta_w^2 \left(1 - \frac{x}{a_{\max}}\right), \tag{20}$$

where $A_t^* = A_t / A_n$.

D. Simulative Calculation of Surface Roughness

After Eq. (13) is solved with practical parameters including Young's modulus and hardness of the diamond abrasive and the RB-SiC, the indentation depth δ_w is obtained, and therefore the simulative calculation of surface roughness is finished. Because it is very difficult for us to totally simulate the RB-SiC surface that is polished by the diamond fixed abrasive, the hypothesis that the surface is formed by the pressure of a still abrasive is accomplished. The indentations that are formed by the still abrasive distribute randomly in the unit area, with the hypothesis above to simulate the surface that is fabricated by pellets. Supposing that the cross section of the indentation is a hemisphere that is upended, the height of the indentation is δ_w. If the position of the same calculation spot is covered by several indentations, the height is the maximum of the indentations. The number of indentations is decided by the number of diamond abrasives involved in the practical fabrication in the unit area. After analysis, the depth of random distribution in the calculating zone is denoted as $z(x_i, y_j)$, and Eq. (21) is used:

$$\mathrm{Ra} = \frac{1}{n^2} \sum_{i=1}^{n} \sum_{j=1}^{n} z(x_i, y_j). \tag{21}$$

The surface roughness of the workpiece is calculated through Eq. (21).

3. Experimental Process and Data Analysis

A. Experimental Process

During the entire experiment, four types of pellets are used (see specifications in Table 2). The pellets that have the same specification are glued on a round cast-iron pad with a diameter of 4 cm, then the pad is mounted on a servo electromotor that has been set to a certain rotation speed and eccentricity. The RB-SiC workpiece is fixed on a platform that has three numerical controlled axes. The RB-SiC workpiece used is manufactured by our institute with a hardness of 30 GPa and a Young's modulus of 330 Gpa. The deionized water is used as coolant.

The fabrication equipment is a FSGJ-1 computer controlled grinding/polishing machine manufactured by CIOMP (Changchun Institute of Optics, fine Machines and Physics, Chinese Academy of Science). The moving mode of the polishing pad is planet motion. Its fastest rotation speed is 200 rpm, the limit of intensity of pressure is 0.5 MPa, and the limit of eccentricity is 10 mm. Figure 3 is a sketch map of the experimental details.

Table 2. Specification of Four Types of Pellets Used in the Experiment

Abrasive Size	W1.5	W3.5	W5	W7
Diameter (mm)	10.0	10.0	10.0	10.0
Thickness (mm)	5.0	5.0	5.0	5.0
Concentration (Diamond Volume Ratio)	3.75%	8.75%	12.5%	17.5%
Resin Type	SP27C	SP27C	SP27C	SP27C
Surface Type	flat	flat	flat	flat

Based on [5–10], we developed an experimental process that is proper for our laboratory. The following are the details of the entire process.

At the beginning of the experimental phase, the residual surface error of the RB-SiC workpiece is obvious. First, W7 pellets are used to grind the RB-SiC workpiece over the entire area. The rotation speed of the principal axis is 80 rpm, the eccentricity is 10 mm, and the pressure intensity is 0.2 Mpa. We expect to achieve a certain shape of surface and, at the same time, to erase the subsurface damage. The surface data from the interferometer are recorded and set as the reference surface. In the next phase, we grind the RB-SiC workpiece over a smaller central

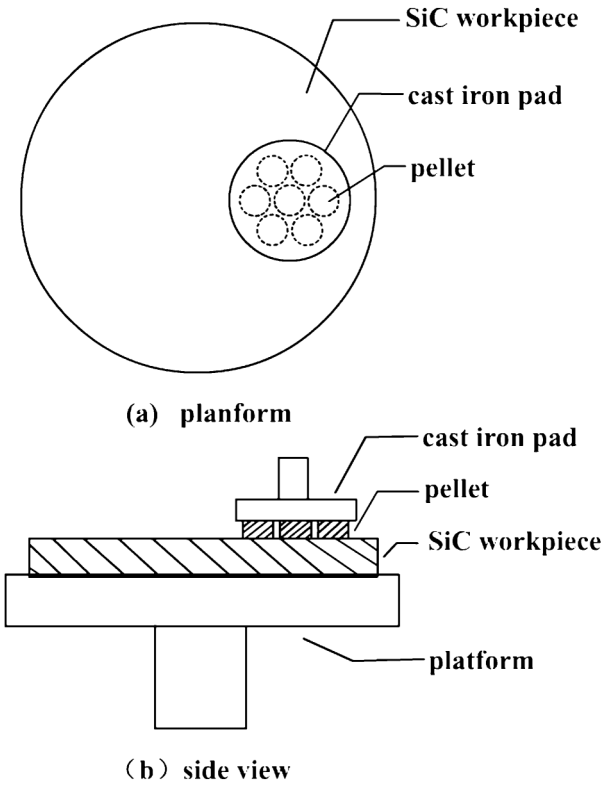

Fig. 3. Sketch of experiment.

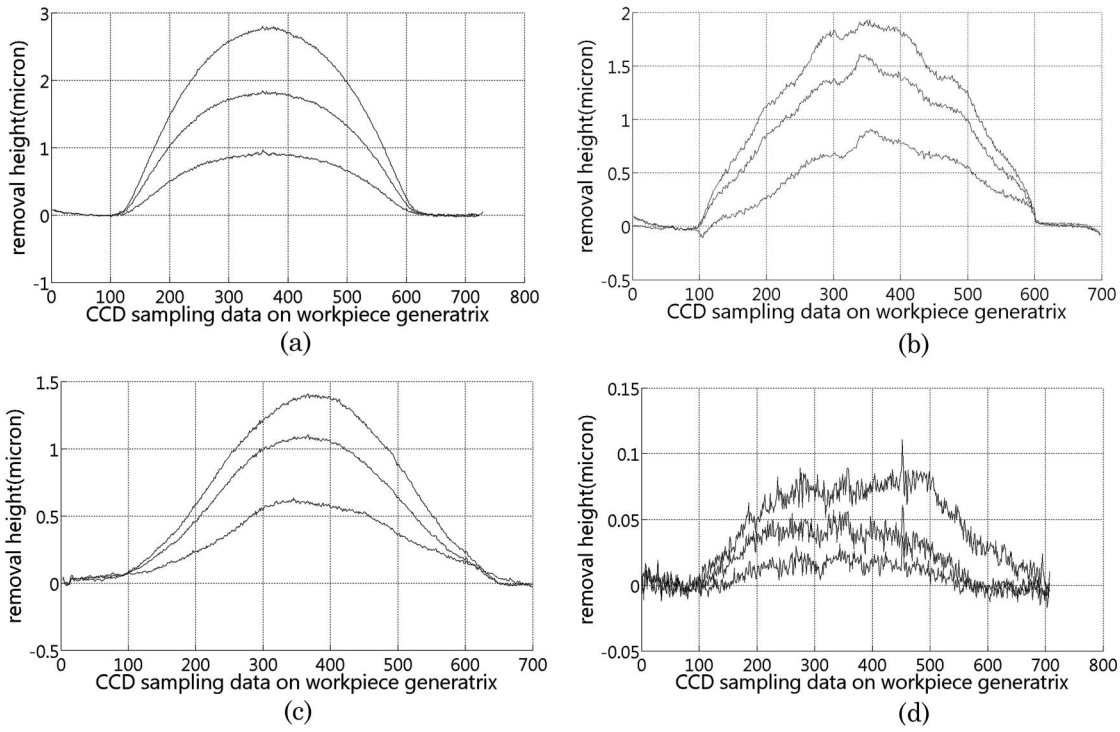

Fig. 4. Curves of material removal with (a) W7 pellet, (b) W5 pellet, (c) W3.5 pellet, and (d) W1.5 pellet.

area. Each fabrication period is 60 min and the period is repeated twice. At the end of the period the data are recorded with a Zygo interferometer. Counting in the reference surface, three group surface data are obtained. Comparison of the three groups' generatrices, which have the same location on the RB-SiC workpiece, are finished and the related removal curves are formed. The W7 pellet removal rate through those curves is acquired. At the end of experiment, the surface roughness in the central area of the RB-SiC workpiece is tested by Dimension 3100 atomic force microscope (AFM). The sample length is 10 μm, and the number of sample points are 256. In the entire process of grinding, any finishing on the pellet surface is not done. Surface roughness of the workpiece reduces as the residual surface error converges.

W5, W3.5, and W1.5 pellets are used to grind/polish the RB-SiC workpiece, respectively, and the procedure described above is repeated. At the end of the whole experiment, the removal rate curves and surface roughness data corresponding to different specifications of pellets are obtained.

B. Experimental Results and Data Analysis

1. *Experimental Results and Analysis of Removal Rate*

According to the experimental process of the removal rate mentioned above, practical values of removal rate with different types of pellets are acquired. The results are displayed in Fig. 4.

Compared with theoretical values, the resulting curves of removal are shown in Fig. 5. The curve with diamond marks in Fig. 5 is theoretical data (the upper curve), the curve with star marks is experimental data (lower curve), and the dashed line is the cubic polynomial fitting curve of the experimental data.

The results of the theory and experiment are analyzed:

1. Figure 5 shows that the corresponding removal rate increases in exponential law as the pellet abrasive diameter increases.
2. The randomicity of the contact area of the practical test in the fabrication process is obvious and the real pellet surface shape is complicated, so it is difficult to simulate the fabricated surface

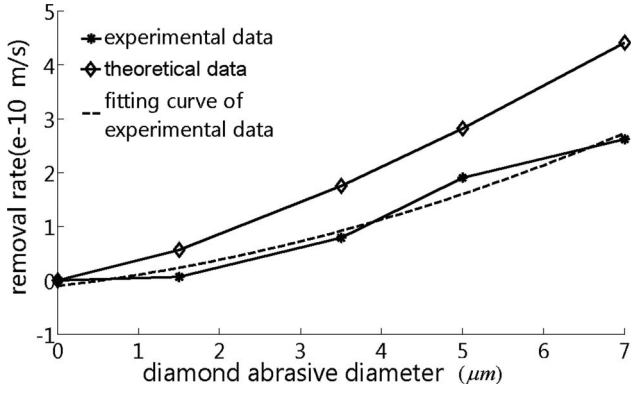

Fig. 5. Removal curve of different types of pellets.

in theory exactly. The only method just approaches the real data as much as possible. In the theoretical curve, the abrasive indentation depth is the maximum depth under certain pressure. However, in the practical situation, lots of abrasive indentations that do not approach its maximum depth exist. So the practical removal rate is smaller than theory; the results are shown in Fig. 5.

3. As shown in the theoretical simulation, in spite of the existence of differences between the experiment and theory, they are all in the same order. The emergence of error is primarily caused by the abrasive indentation, but there are many other practical factors that affect the removal rate. Only the pressure on the pellets, the velocity of the polishing pad, and the abrasive concentration are considered in the model. In the practical situation other unpredictable factors also cause the error between experiment and theory.

4. In the model, removal rate is positively proportional to the square of the indentation depth. In other words, removal rate is positively proportional to the square of the pressure on the abrasive. The situation is different from the Preston function in which the removal rate is only positively proportional to pressure. So the result is analyzed: the loose diamond abrasive movement rolls in the fabrication process and the fixed abrasive movement slips. The different movement states are mainly the cause of disagreement between theory and traditional Preston function. Further detailed analysis should be based on sufficient experimental data.

5. Equation (13) is solved; the result shows that A_i^* and δ_w/D are all constant. So only the abrasive concentration in the pellet and the rotation speed of the polishing pad have an obvious influence on the material removal rate.

2. *Experimental Results and Analysis of Surface Roughness*

In the experiment of surface roughness measurement, the equipment used is a Dimension 3100 AFM manufactured by DI company. Its sample length is 10 μm. The sample spot number is 256. The results are displayed in Fig. 6.

The combination of the indentation depth model from Eq. (13) and surface roughness model from Eq. (21) is finished, and theoretical surface roughness results are gained. Compared with the experimental results, the following conclusions are achieved in Fig. 7. The curve with diamond marks in Fig. 7 is the theoretical data and the curve with star marks is the experimental data.

The analysis results are concluded:

1. According to the comparison of theory and experiment, the general trend of the surface roughness curve is obtained: the workpiece surface roughness

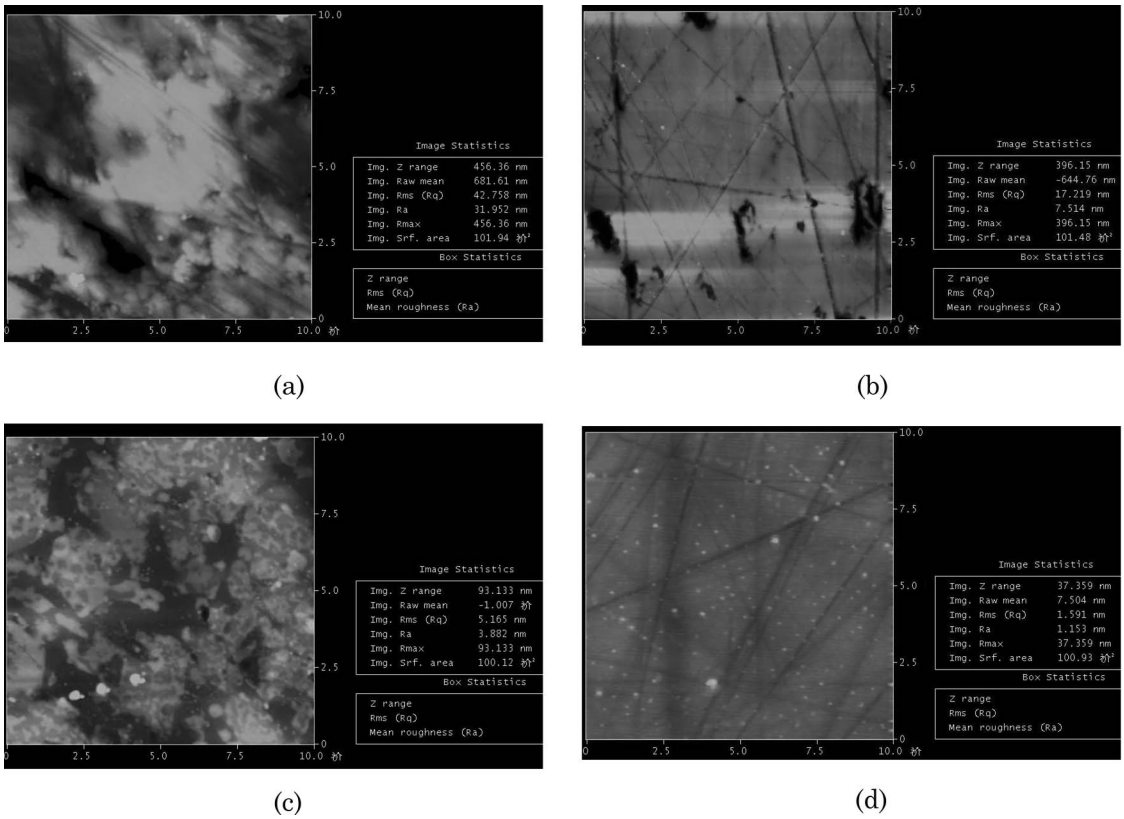

Fig. 6. Comparison of AFM testing results: (a) W7 fabricating result, Ra = 31.952 nm; (b) W5 fabricating result, Ra = 7.514 nm; (c) W3.5 fabricating result, Ra = 3.882 nm; (d) W1.5 fabricating result, Ra = 1.151 nm.

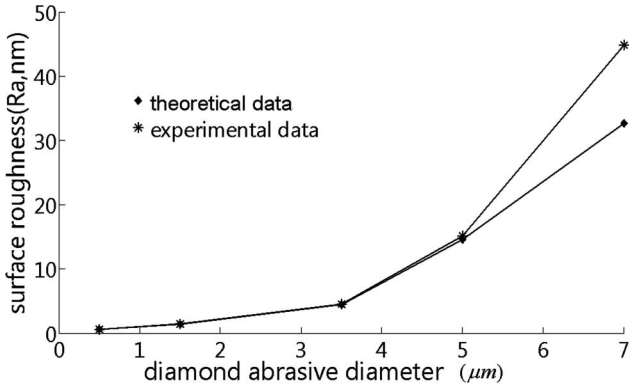

Fig. 7. Surface roughness curve of different type pellets.

increases nonlinearly as the abrasive diameter increases.

2. In Fig. 7, the experimental results are bigger than theory. The ratio of error between the experiment and theory is 5.97%, 3.19%, 3.59%, and 37.37%, respectively. The primary cause of the error is that many larger diameter abrasives exist in the pellets, which make the workpiece surface roughness larger than theory. However, in the simulating process it is supposed that the abrasive diameter uniformity is much better.

3. Under the precondition that the experimental results are bigger than the theoretical, the result of the W7 pellet is much more obvious as the ratio of error approaches 37.37%. The main cause of the error is that: there are many more abrasives with a diameter over 7 μm existing in the W7 pellets, and RB-SiC material removal is brittleness removal, which means the phenomenon of material crack exists. So the material crack, which has serious influence on surface roughness, causes deeper indentation than that of the theoretical prediction.

4. In Figs. 6(b) and 6(d), the scratch on the workpiece surface is extremely obvious. It is caused by two reasons:

1. Many more abrasives with a diameter larger than the standard abrasive diameter of W5 and W1.5 pellets, which easily causes the scratches on the workpiece surface in the working process. So the procedures that filter the diamond abrasive should be much stricter during pellet manufacturing.

2. Not clearing the flotsam left in the last working procedure also causes the emergence of scratch on the workpiece surface. So the cleaning work among different working procedures should be finished strictly and carefully.

4. Conclusion

In this paper we have given a detailed theoretical analysis and simulation of fixed abrasive technology in a microcosm and introduced the basic technology procedure that fabricates RB-SiC workpieces. The removal rate experimental results display that the removal rate increases in nonlinear law as the abrasive diameter increases. Compared with the data obtained from the experiment, the experimental removal rate is a little lower than theory, but the error is controlled in the same quantitative order. In the surface roughness experiment, a smooth surface whose roughness is Ra 1.151 nm is achieved by a W1.5 pellet. The data of the experiment and theory match very well in the comparison process.

The fixed abrasive fabrication principle decides that the stability of the removal rate of technology is very good in the fabrication process, and the theoretical model matches well with experimental results, making the model useful in practical application. In the surface roughness experiment, compared with traditional loose abrasive technology, the same surface quality is obtained by fixed abrasive technology with a bigger abrasive. Because of the high fabrication efficiency and low cost of fixed abrasive technology, it has wide application possibilities in the field of fabricating RB-SiC mirrors.

References

1. M. A. Ealey and G. Q. Weaver, "Developmental history and trends for reaction bonded silicon carbide mirrors," Proc. SPIE **2857**, 66–72.
2. Y. Zhao, D. M. Maietta, and L. Chang, "An asperity micro-contact model incorporating the transition from elastic deformation to fully plastic flow," J. Tribol. **122**, 86–93 (2000).
3. Y. Zhao and L. Chang, "A micro-contact and wear model for chemical-mechanical polishing of silicon wafers," Wear **252**, 220–226 (2002).
4. E. Rabinowicz, *Friction and Wear of Materials*, 2nd ed. (Wiley, 1995).
5. D. Xue, Z. Zhang, and X. Zhang, "Computer controlled polishing technology for middle or small aspheric lens," Opt. Precision Eng. **13**, 198–204 (2005).
6. H. Y. Tam, H. B. Cheng, and Y. W. Wang, "Removal rate and surface roughness in the lapping and polishing of RB-RB-SiC optical components," J. Mater. Process. Technol. 192–193, 276–280 (2007).
7. X. Zhang, Y. Zhang, and J. Yu, "FSGJ-1 system of asphere automaking and on-line testing," Opt. Precision Eng. **5**, 70–76 (1997).
8. L. Zheng, X. Zhang, and F. Zhang, "NC surfacing of two off-axis aspheric mirrors," Opt. Precision Eng. **12**, 113–117 (2004).
9. J. Yang and C. Tian, *High Speed Lapping Technology* (Academic, 2003).
10. D. F. Edwards and P. P. Hed, "Optical glass fabrication technology. 1: Fine grinding mechanism using bound diamond abrasives," Appl. Opt. **26**, 4670–4676 (1987).